AIP | Applied Physics Letters

Phonon dynamics in CuxBi2Se3 (x=0, 0.1, 0.125) and Bi2Se2 crystals studied using femtosecond spectroscopy

H.-J. Chen, K. H. Wu, C. W. Luo, T. M. Uen, J. Y. Juang, J.-Y. Lin, T. Kobayashi, H.-D. Yang, R. Sankar, F. C. Chou, H. Berger, and J. M. Liu

Citation: Applied Physics Letters **101**, 121912 (2012); doi: 10.1063/1.4754005
View online: http://dx.doi.org/10.1063/1.4754005
View Table of Contents: http://scitation.aip.org/content/aip/journal/apl/101/12?ver=pdfcov
Published by the AIP Publishing

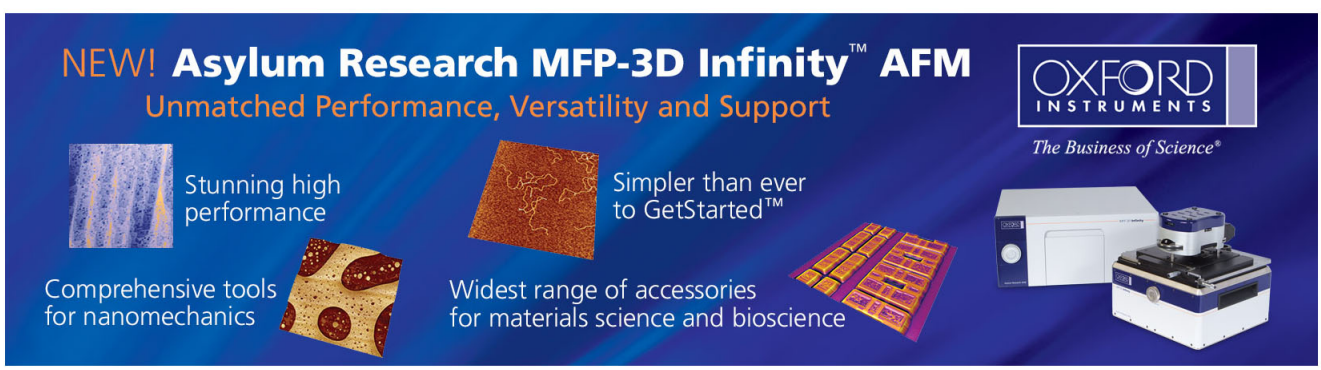

Phonon dynamics in $Cu_xBi_2Se_3$ (x = 0, 0.1, 0.125) and Bi_2Se_2 crystals studied using femtosecond spectroscopy

H.-J. Chen,[1] K. H. Wu,[1,a)] C. W. Luo,[1] T. M. Uen,[1] J. Y. Juang,[1] J.-Y. Lin,[2] T. Kobayashi,[1] H.-D. Yang,[3] R. Sankar,[4] F. C. Chou,[4] H. Berger,[5] and J. M. Liu[6]
[1]*Department of Electrophysics, National Chiao Tung University, Hsinchu 300, Taiwan*
[2]*Institute of Physics, National Chiao Tung University, Hsinchu 300, Taiwan*
[3]*Department of Physics, National Sun Yat-sen University, Kaohsiung 804, Taiwan*
[4]*Center for Condensed Matter Sciences, National Taiwan University, Taipei 106, Taiwan*
[5]*Institute of Physics of Complex Matter, École polytechnique fédérale de Lausanne, Switzerland*
[6]*Department of Electrical Engineering, University of California, Los Angeles, California 90095, USA*

(Received 7 June 2012; accepted 5 September 2012; published online 19 September 2012)

Phonon dynamics in Bi, Bi_2Se_2, and $Cu_xBi_2Se_3$ (x = 0, 0.1, 0.125) single crystals was investigated using femtosecond pump-probe spectroscopy. Two damped oscillations in measured transient reflectivity changes were observed, respectively, attributed to coherent optical and acoustic phonons. The frequency shift of the phonon modes in Bi-rich Bi_2Se_2 crystals indicates the intercalation of the additional Bi atoms into the Bi_2Se_3 matrix and formation of the Bi_2 layer between the quintuple layers (QLs). The deformation of QLs in $Cu_xBi_2Se_3$ crystals was also found. These phonon dynamics results suggest that Cu atoms in $Cu_xBi_2Se_3$ crystals are predominantly intercalated between pair of QLs. © *2012 American Institute of Physics*. [http://dx.doi.org/10.1063/1.4754005]

Topological insulators (TIs) are recently discovered states of quantum matter characterized by a full gap with degenerated spins in the bulk while exhibiting polarized spins and no gap on the surface.[1,2] The salient electronic, optical, and magnetic properties of these materials provide innovative opportunities not only for research in fundamental physics but also for potentially revolutionary applications such as quantum computers and spintronic devices.[1–3] Bi-based compounds such as Bi_2Se_3 and Bi_2Te_3 have been extensively investigated due to their intriguing thermoelectric properties and their uniqueness of being three-dimensional TIs. Recently, the effect of doping atoms is one of the most important issues for Bi-based TIs. Previous research showed that the "robust" conducting edge states did not disappear even when some impurity atoms are doped into TIs.[4–7] The doping atoms can also induce significant modification on surface electronic states, such as opening up a gap at the Dirac point[4] and shifting the Fermi level.[5] Moreover, Bi-based TIs doped with Fe, Mn, and Cr can exhibit other interesting physical properties, such as ferromagnetism[8,9] and anomalous quantized Hall effect,[10] while superconductivity has been observed in Bi-based TIs doped with Cu.[6,7] Recent investigations on superconductivity exhibited in $Cu_xBi_2Se_3$ provide the platforms for studying the interplay between topological and broken-symmetry order.[6] However, the locations of the doped Cu atoms still remain a subject of debate. The Cu atoms can either be intercalated between van der Waals-like bonded Se planes or substitute Bi atoms in the lattice[7]; these two different possibilities cause different structural deformations in the Bi_2Se_3 matrix. Previous studies on Bi_2Te_3 also indicate that application of extra pressure on the sample can induce superconductivity while the topological surface states remain well defined.[11,12] Furthermore, it has been demonstrated that small changes in lattice parameters and atomic positions in Bi_2Te_3 can result in surface states that are slightly different from those in the original Bi_2Te_3.[11] This calculation result implies that the structural strain might be relevant to the superconductivity observed in some TIs. Thus, in order to understand the underlying mechanism that gives rise to superconductivity in $Cu_xBi_2Se_3$, it is essential to investigate the changes in crystal structure that are caused by the doped Cu atoms. Such changes in crystal structure can be studied by probing the changes in phonon dynamics using ultrafast spectroscopy.

Bi_2Se_3 is a narrow-gap semiconductor with a rhombohedral crystal structure belonging to the $D_{3d}^5(R\bar{3}m)$ space group. The Bi_2Se_3 crystal structure is constructed by repeated quintuple layers (QLs) arranged along the *c* axis. Each QL is stacked in a sequence of Se(1)-Bi-Se(2)-Bi-Se(1) atomic layers and is weakly bonded to its neighboring QLs by van der Waals interaction. This property makes the native Bi_2Se_3 crystal a layered compound such that both substitution and intercalation can take place for a small percentage of foreign atoms added into this material. For example, the crystal structure of a Bi-rich Bi-Se compound, Bi_2Se_2, is similar to that of Bi_2Se_3, but it has a bi-layer Bi-Bi slab inserted between two QLs.[13,14] That is, the additional Bi atoms are intercalated into the Bi_2Se_3 matrix to form the Bi_2 layers. In this case, each QL will feel an extra Coulomb force resulted from the layer of doped atoms. This Coulomb interaction distorts the structure of the QL by changing its bond length and bond angle. Moreover, because this interaction also suppresses the original vibration of the QL, the corresponding phonon dynamics of the QL is changed slightly. As we will show later, it causes a red shift in the phonon frequency for the intercalation case. In addition to intercalation, the doped atoms can also substitute the Bi atom inside the QL. Previous Raman scattering studies on rhombohedral V_2-VI_3 compounds reveal a blue shift in the phonon frequency when the lighter Sb atom substitutes Bi atom in the QL of $Bi_{2-y}Sb_yTe_3$.[10] Clearly, composition change in the QL also affects the phonon dynamics.

a)Electronic mail: khwu@cc.nctu.edu.tw.

Because the phonon frequency shift caused by substitution and that caused by intercalation have opposite signs, the structural deformation and the locations of doped atoms in a TI can be resolved by measuring the sign and magnitude of the phonon frequency shift.

Ultrafast time-resolved pump-probe spectroscopy has proven to be a powerful tool in unraveling the carrier, lattice, and spin dynamics in various materials. An ultrashort laser pulse that is sufficiently shorter than the period of a particular vibrational mode can excite the mode with a high degree of temporal and spatial coherence in a material. Therefore, propagation and localization of coherent phonons can be observed directly in the time domain.[15,16] Recently, coherent phonons generated by ultrashort laser pulses have been observed in a wide variety of materials, such as semiconductors, metals, superconductors, colossal magnetoresistive manganites, and multiferroics.[17–21] Both coherent optical phonons (COPs) and coherent acoustic phonons (CAPs) have been measured in thermoelectric materials and topological insulators, such as Sb_2Te_3,[22,23] Bi_2Te_3,[24] and Bi_2Se_3.[25,26] Because the COPs measured in femtosecond pump-probe spectroscopy are Raman active, the corresponding COP frequency should show up in conventional Raman spectra. Indeed, in previous studies performed on rhombohedra1 V_2-VI_3 compounds[22–26] using ultrafast pump-probe experiments, a damped oscillation of a subpicosecond period that is observed in measured transient variations of reflectivity or transmission ($\Delta R/R$ or $\Delta T/T$) is attributed to the displacive excitation of COPs associated with the Raman active modes. Another damped oscillation of a longer period of tens of picoseconds, originally identified by Thomsen *et al.*,[15] is attributed to the CAP oscillations generated by the interference of the probe beams reflected from the sample surface and the strain pulse that propagates longitudinally at sound velocity. The relationship between the period τ_f of the slow oscillation and the longitudinal sound velocity v_s is $\tau_f = \lambda/[2v_s(\sqrt{n^2 - \sin^2\theta})]$, where λ is the probe wavelength, n is the refractive index at λ, and θ is the incident angle of the probe beam. Consequently, one can obtain the sound velocity by measuring the CAP oscillations provided that the refractive index of the material is known.

In the present study, we use optical-pump optical-probe femtosecond time-domain spectroscopy to investigate the dynamics of coherent phonons in Bi, Bi_2Se_2, and $Cu_xBi_2Se_3$ ($x = 0$, 0.1, 0.125) single crystals. Two damped oscillations, namely the fast and slow oscillation components, in the measured $\Delta R/R$ curves are observed in these samples and are attributed to COP and CAP, respectively. Analyses carried out on the COP oscillation (the fast component) in the Bi_2Se_2 crystal reveal that the shift of the A_{1g} phonon mode frequency of the Bi layer and that of the QL have opposite signs and are respectively associated with the shortening and stretching of the bond/chain length. The deformation of the QL in $Cu_xBi_2Se_3$ crystals is also clearly observed. The structural deformation and the shift of the $A_{1g}{}^1$ phonon frequency associated with the effects resulted from the doped Cu atoms are discussed. From the phonon frequency shifts and the lifetime of the COP, the locations of the Cu atoms in $Cu_xBi_2Se_3$ can be determined, and the influence of the Cu atoms in QL is subsequently resolved.

Single crystal samples of $Cu_xBi_2Se_3$ ($x = 0$, 0.1, 0.125), Bi_2Se_2, and Bi have been prepared using stoichiometric mixtures of 5 N purity of Bi, Se, and Cu in sealed evacuated quartz tubes. Bi crystals were grown by vertical Bridgman method between 450 and 270 °C of thermal gradient of ~1 °C/cm near solidification point with a pulling rate of 0.1 mm/h. $Cu_xBi_2Se_3$ crystals were grown with slow-cooling method from 850 °C to 650 °C at a rate of 2 °C/h and then quenched in cold water. Single crystal Bi_2Se_2 has been prepared using vertical Bridgman method. Preliminary homogenization was carried out in a horizontal tube furnace at 350 °C for 75 h. The sealed ampoules were then passed through a vertical Bridgman furnace between 650 and 600 °C of thermal gradient ~1 °C/cm near the solidification point. The pulling rate was kept at 0.2 mm/h. The resulting crystals could be cleaved easily, and the freshly cleaved plane showed a silvery shining mirror-like surface. All of the samples were kept in a vacuum tank to avoid surface oxidation. Before each experiment, the sample was cleaved using a scotch tape to ensure that a flat and reflective surface was obtained. Figure 1 shows the x-ray diffraction patterns of Bi, Bi_2Se_2, and $Cu_xBi_2Se_3$ ($x = 0$, 0.1, 0.125) single crystals. The diffraction peaks reveal pure (00*l*)-oriented reflections without any discernible impurity phase, indicating that all the single crystal samples have a pure *c*-axis oriented normal to the cleaved surface.

For standard pump-probe measurements, a commercial mode-locked Ti:sapphire laser system providing ultrashort pulses of 100 fs-pulsewidth at a repetition rate of 5 MHz and a center wavelength of 800 nm was used. The fluences of the pump beam and the probe beam were 1 mJ/cm^2 and 0.067 mJ/cm^2, respectively. The pump beam was focused on the $Cu_xBi_2Se_3$ single crystals to a diameter of 35 μm, and the probe beam was focused to a diameter of 25 μm at the center of the pump beam spot. The polarizations of the pump and probe beams were orthogonal to each other and were perpendicular to the *c*-axis of the $Cu_xBi_2Se_3$ single crystals. All the samples were stuck on a copper sample holder in a cryostat and kept at a constant temperature of 293 K before laser illumination. A linear motor stage was used to vary the delay time between the pump and probe pulses. The small reflected signals were detected by using a photodiode and a lock-in amplifier.

Figures 2(a)–2(e) display the typical $\Delta R/R$ signals as a function of delay time for all samples measured at room

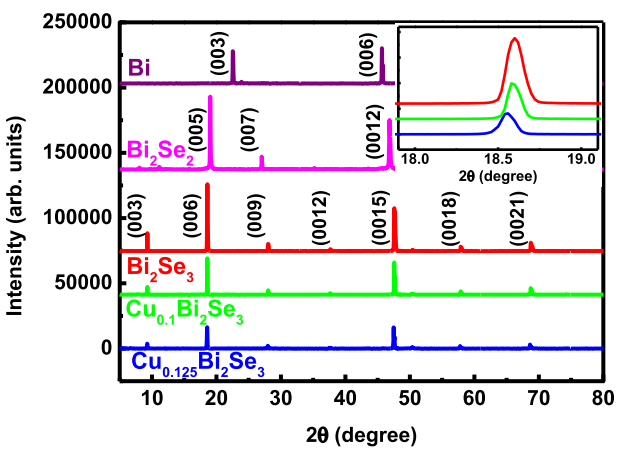

FIG. 1. X-ray diffraction patterns of Bi, Bi_2Se_2, and $Cu_xBi_2Se_3$ ($x = 0$, 0.1, 0.125) crystals. Inset: Magnified patters around the (006) peak of $Cu_xBi_2Se_3$.

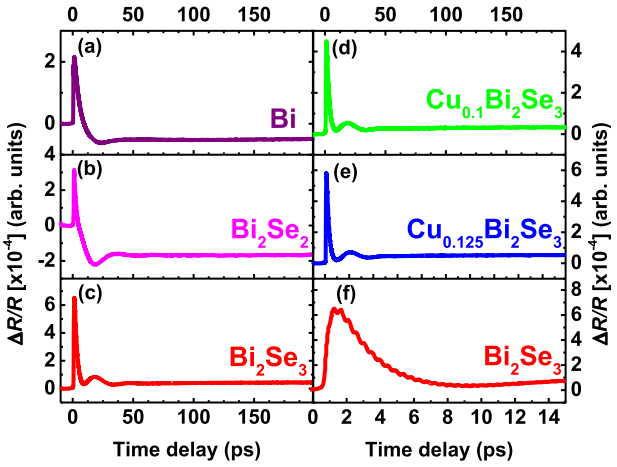

FIG. 2. Temporal variations of $\Delta R/R$ signals for (a) Bi, (b) Bi_2Se_2, (c) Bi_2Se_3, (d) $Cu_{0.1}Bi_2Se_3$, and (e) $Cu_{0.125}Bi_2Se_3$ crystals at room temperature for the pump-probe energy 1.55 eV. (f) $\Delta R/R$ signal of Bi_2Se_3 crystal observed on a short timescale. Note that the horizontal time scale for panel (f) is different from the other panels.

temperature. In general, the time evolution of each $\Delta R/R$ curve can be separated into several components corresponding to different energy-transfer processes: A fast component of a sub-picosecond time scale characterizes the thermalization between electrons and optical phonons, while a subsequent slow component of a time scale of several picoseconds characterizes the thermalization between electrons and acoustic phonons.[26] After the electron-lattice relaxation through these processes, a quasi-constant component is observed, which might represent heat diffusion out of the illuminated area on the sample.[25] In addition, two damped oscillation components of different periods are superimposed on the $\Delta R/R$ curves. Only the slow oscillations can be seen in Figures 2(a)–2(e) because the $\Delta R/R$ signals in these figures are plotted on long timescales. The fast oscillation component of a Bi_2Se_3 crystal is shown in Figure 2(f). This component can be extracted by removing the adjacent average background from the measured $\Delta R/R$ signal; the result is displayed in Figure 3(c). The frequency of this component is centered at 2.148 THz; it can be assigned as the A_{1g}^1 COP

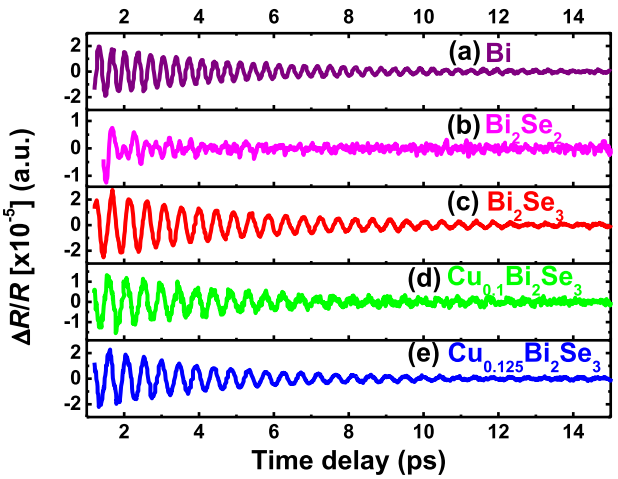

FIG. 3. High-frequency oscillatory temporal variations of $\Delta R/R$ signals for all samples: (a) Bi crystal, (b) Bi_2Se_2 crystal, (c) Bi_2Se_3 crystal, (d) $Cu_{0.1}Bi_2Se_3$ crystal, (e) $Cu_{0.125}Bi_2Se_3$ crystal.

mode of Bi_2Se_3, based on comparison with continuous-wave (CW) Raman spectroscopy.[27] The slow oscillation components, as shown in Figures 2(a)–2(e), are attributed to the CAPs generated by ultrafast laser pulses. The frequency of the CAP for the Bi_2Se_3 crystal is centered at 0.033 THz (the corresponding period is ~30 ps), and the oscillation decays completely within ~60 ps. According to the pulse strain model, the disappearance of the slow oscillation around 60 ps is determined by the penetration depth of the probe beam at 800 nm. Taking the refractive index of Bi_2Se_3 crystal reported in Ref. 28, the sound velocity is estimated to be 1996.33 m/s at room temperature. Figures 2(c)–2(e) also reveal that the periods of the slow oscillations of $Cu_xBi_2Se_3$ (x = 0, 0.1, 0.125) crystals vary slightly (from 29.9 ps to 30.2 ps). By contrast, the frequencies of the fast oscillations display a significantly distribution among the samples studied and are associated with the changes in the chain length of the QL and in the lattice constant *c*. Thus, in the following we concentrate on the COP behaviors exhibited by the Bi, Bi_2Se_2, and $Cu_xBi_2Se_3$ (x = 0, 0.1, 0.125) single crystals and attempt to clarify the changes in the crystal structure of Cu-doped Bi_2Se_3.

Figures 3(a)–3(e) show the fast oscillation component for each single crystal. For the Bi_2Se_2 crystal, shown in Figure 3(b), the strength of the oscillatory signal is significantly smaller and its relaxation time much shorter than those for the other crystals. Besides, this oscillatory signal also exhibits a complex behavior in the first few picoseconds. To understand this complex oscillation, we use the methods of short time Fourier transformation (STFT)[29–31] and fast Fourier transformation (FFT) to analyze the oscillatory signals. A Blackman window with a full-width at half-maximum (FWHM) of 2400 fs was used as a gate function in the STFT calculation.[30] Figures 4(a)–4(e) display the STFT spectra of the oscillatory signals shown in Figures 3(a)–3(e), respectively. As is evident from Figure 4(b), two characteristic peaks centered at 2.025 THz and 3.319 THz are observed for the Bi_2Se_2 crystal, which are respectively very close to the A_{1g}^1 mode frequencies of the Bi (Figure 4(a)) and Bi_2Se_3 (Figure 4(c)) crystals. However, both peaks are slightly shifted away from the characteristic frequencies of the A_{1g}^1 mode in pure Bi and Bi_2Se_3 crystals. These shifts of the spectral peaks can be explained by the changes in bond lengths due to the involvement of a covalent contribution into the bonding between the Se-Bi-Se-Bi-Se five-layer slab and the Bi-Bi two-layer slab in the Bi_2Se_2 crystal.[13,14] By comparison to pure Bi and Bi_2Se_3 crystals, this additional covalent contribution rebalances the distance and angle of the Bi-Bi bonds and the Se-Bi-Se-Bi-Se chains. The chain length of Se-Bi-Se-Bi-Se QL stretches from 11.752 Å in Bi_2Se_3 to 11.797 Å in Bi_2Se_2 (Ref. 14) such that the A_{1g}^1 mode frequency of the QL layer structure decreases from 2.148 THz in a Bi_2Se_3 crystal to 2.025 THz in a Bi_2Se_2 crystal. By contrast, the bond length of the Bi-Bi bond in Bi_2Se_2 shortens from 3.056 Å in Bi to 2.987 Å in Bi_2Se_2 (Ref. 14) such that the A_{1g}^1 mode frequency of the Bi_2 layer structure increases from 2.928 THz in a Bi crystal to 3.319 THz in a Bi_2Se_2 crystal. For the Se-Bi-Se-Bi-Se chain, the frequency shift is −0.123 THz for a 0.38% change in the chain length, while for the Bi-Bi bond, the frequency shift is 0.391 THz for a

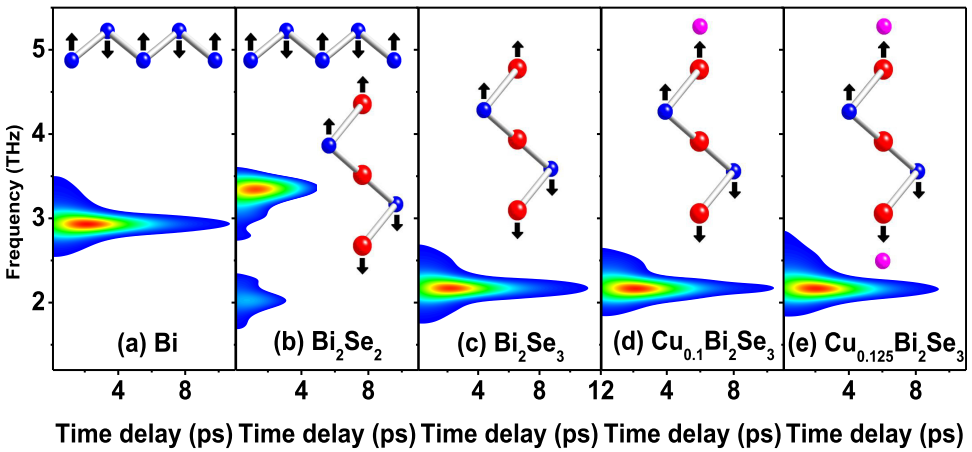

FIG. 4. STFT spectrograms of high-frequency oscillatory signals for all samples: (a) Bi crystal, (b) Bi_2Se_2 crystal, (c) Bi_2Se_3 crystal, (d) $Cu_{0.1}Bi_2Se_3$ crystal, (e) $Cu_{0.125}Bi_2Se_3$ crystal. Schematic diagrams of the Raman A_{1g}^1 modes for the samples are also shown (Bi atoms are shown in blue, Se in red and Cu in pink).

−2.26% change in the bond length. These results indicate that in Bi_2Se_2, where extra Bi atoms are intercalated between QLs, the phonon frequency of the A_{1g}^1 mode of the QL exhibits a red shift compared to that in Bi_2Se_3. Therefore, it appears that the microstructural deformation in the Bi_2Se_2 crystals can be accurately resolved by measuring the magnitude and sign of the phonon frequency shift of the QL.

Figures 4(d) and 4(e) are the STFT spectra for the $Cu_{0.1}Bi_2Se_3$ and $Cu_{0.125}Bi_2Se_3$ crystals, respectively. The STFT spectra reveal that the lifetime of the A_{1g}^1 phonon mode decreases with increasing Cu concentration. In order to quantitatively analyze this behavior, a damped oscillation waveform $A_{\mathrm{osc}}\cos(2\pi f_{\mathrm{osc}}t+\phi)e^{-t/\tau_{\mathrm{dephasing}}}$ was used to fit the original data shown in Figure 3 to get the dephasing time ($\tau_{\mathrm{dephasing}}$) and the phonon frequency (f_{osc}) for samples of various Cu concentrations. Figure 5 shows the fitting results obtained from samples of various Cu concentrations. These results show that both the phonon frequency and the dephasing time decrease with increasing Cu concentration, indicating that the addition of Cu atoms does indeed deform the Se-Bi-Se-Bi-Se chain in $Cu_xBi_2Se_3$ crystals, even though this deformation is much smaller than that in Bi_2Se_2 crystals. The inverse relation between the phonon frequency and the Cu concentration provides us with the information about the locations of the Cu atoms. As mentioned above, for the substitution case where a Bi atom is replaced by a doping atom, the Raman spectrum reveals that the phonon frequency of the A_{1g}^1 mode increases with increasing doping concentration, while for the intercalation case where a doping atom is intercalated between two QLs, the phonon frequency of the A_{1g}^1 mode decreases with increasing doping concentration. Therefore, the photon frequency shifts seen in Figure 5 for $Cu_xBi_2Se_3$ crystals hint at intercalation for the Cu atoms. Additionally, as also shown in Figure 5, the lattice constant c increases slightly with increasing Cu concentration, implying that the QL chain in $Cu_xBi_2Se_3$ is stretched by the doping Cu atoms. The stretch of the QL chain length can be interpreted as follows: When the doping Cu atoms are intercalated between QLs, they form a mediated layer to strengthen the interaction between QLs instead of the weak van der Waals interaction, thus stretching the chain length of the QL. It is reasonable to conclude from our experimental results that the Cu atoms are intercalated between every pair of QLs, and these intercalated Cu atoms cause an effective interaction to slightly deform the QLs.

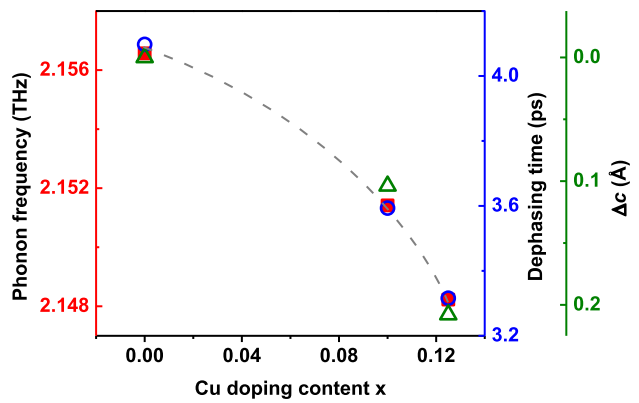

FIG. 5. Phonon frequency (red square) and dephasing time of A_{1g}^1 phonon mode (blue circle) and change in lattice constant c (green triangle) for $Cu_xBi_2Se_3$ crystal as a function of Cu doping concentration.

In conclusion, we have systematically studied the A_{1g}^1 COP dynamics in Bi, Bi_2Se_2, and $Cu_xBi_2Se_3$ (x = 0, 0.1, 0.125) single crystals using femtosecond pump-probe reflectivity spectroscopy. Because the phonon frequency shift caused by substitution and that caused by intercalation have opposite signs, the structural deformation and the locations of the doping atoms in a TI can be resolved by measuring the sign and magnitude of the phonon frequency shift. The frequency shifts of the phonon modes in Bi-rich Bi_2Se_2 crystals indicate that the extra Bi atoms are intercalated into the Bi_2Se_3 matrix and form a Bi_2 layer between the QLs. From the red shift of the A_{1g}^1 phonon frequency associated with the doping of Cu atoms, we also conclude that the additional Cu atoms are predominantly intercalated between every pair of QLs in $Cu_xBi_2Se_3$ crystals. The relationship between structural deformation and superconductivity, however, needs further investigations; in particular, the temperature-dependent phonon dynamics in $Cu_xBi_2Se_3$ crystals are crucial for understanding this relationship. Experimental work along these directions is in progress.

This project is financially sponsored by the National Science Council (Grant Nos. NSC 98-2112-M-009-006-MY3 and NSC 98-2112-M-009-008-MY3) and the Ministry of Education (2011 MOE ATU program at NCTU) of Taiwan, R.O.C.

[1]M. Z. Hasan and C. L. Kane, Rev. Mod. Phys. **82**, 3045 (2010).
[2]X.-L. Qi and S.-C. Zhang, Rev. Mod. Phys. **83**, 1057 (2011).

[3]Q.-K. Xue, Nat. Nanotechnol. **6**, 197 (2011).
[4]L. A. Wray, S.-Y. Xu, Y. Xia, D. Hsieh, A. V. Fedorov, Y. S. Hor, R. J. Cava, A. Bansil, H. Lin, and M. Z. Hasan, Nat. Phys. **7**, 32 (2011).
[5]D. Hsieh, Y. Xia, D. Qian, L. Wray, J. H. Dil, F. Meier, J. Osterwalder, L. Patthey, J. G. Checkelsky, N. P. Ong, A. V. Fedorov, H. Lin, A. Bansil, D. Grauer, Y. S. Hor, R. J. Cava, and M. Z. Hasan, Nature (London) **460**, 1101 (2009).
[6]L. A. Wray, S.-Y. Xu, Y. Xia, Y. S. Hor, D. Qian, A. V. Fedorov, H. Lin, A. Bansil, and M. Z. Hasan, Nat. Phys. **6**, 855 (2010).
[7]Y. S. Hor, A. J. Williams, J. G. Checkelsky, P. Roushan, J. Seo, Q. Xu, H. W. Zandbergen, A. Yazdani, N. P. Ong, and R. J. Cava, Phys. Rev. Lett. **104**, 057001 (2010).
[8]Y. S. Hor, P. Roushan, H. Beidenkopf, J. Seo, D. Qu, J. G. Checkelsky, L. A. Wray, D. Hsieh, Y. Xia, S.-Y. Xu, D. Qian, M. Z. Hasan, N. P. Ong, A. Yazdani, and R. J. Cava, Phys. Rev. B **81**, 195203 (2010).
[9]T. M. Schmidt, R. H. Miwa, and A. Fazzio, Phys. Rev. B **84**, 245418 (2011).
[10]R. Yu, W. Zhang, H.-J. Zhang, S. C. Zhang, X. Dai, and Z. Fang, Science **329**, 61 (2010).
[11]J. L. Zhang, S. J. Zhang, H. M. Weng, W. Zhang, L. X. Yang, Q. Q. Liu, S. M. Feng, X. C. Wang, R. C. Yu, L. Z. Cao, L. Wang, W. G. Yang, H. Z. Liu, W. Y. Zhao, S. C. Zhang, X. Dai, Z. Fang, and C. Q. Jin, Proc. Natl. Acad. Sci. **108**, 24 (2011).
[12]C. Zhang, L. Sun, Z. Chen, X. Zhou, Q. Wu, W. Yi, J. Guo, X. Dong, and Z. Zhao, Phys. Rev. B **83**, 140504(R) (2011).
[13]H. Lind and S. Lidin, Solid State Sci. **5**, 47 (2003).
[14]H. Lind, S. Lidin, and U. Häussermann, Phys. Rev. B **72**, 184101 (2005).
[15]C. Thomsen, H. T. Grahn, H. J. Maris, and J. Tauc, Phys. Rev. B **34**, 4129 (1986).
[16]H. J. Zeiger, J. Vidal, T. K. Cheng, E. P. Ippen, G. Dresselhaus, and M. S. Dresselhaus, Phys Rev. B **45**, 768 (1992).
[17]A. V. Bragas, C. Aku-Leh, S. Costantino, A. Ingale, J. Zhao, and R. Merli, Phys. Rev. B **69**, 205306 (2004).
[18]R. N. Kini, A. J. Kent, N. M. Stanton, and M. Henini, Appl. Phys. Lett. **88**, 134112 (2006).
[19]I. Matsubara, S. Ebihara, T. Mishina, and J. Nakahara, Phys. Rev. B **79**, 054110 (2009).
[20]Y. H. Ren, M. Trigo, R. Merlin, V. Adyam, and Q. Li, Appl. Phys. Lett. **90**, 251918 (2007).
[21]H. C. Shih, L. Y. Chen, C. W. Luo, K. H. Wu, J.-Y. Lin, J. Y. Juang, T. M. Uen, J. M. Lee, J. M. Chen, and T. Kobayashi, New J. Phys. **13**, 053003 (2011).
[22]Y. Wang, X. Xu, and R. Venkatasubramanian, Appl. Phys. Lett. **93**, 113114 (2008).
[23]Y. Li, V. A. Stoica, L. Endicott, G. Wang, C. Uher, and R. Clarke, Appl. Phys. Lett. **97**, 171908 (2010).
[24]N. Kamaraju, S. Kumar, and A. K. Sood, Europhys. Lett. **92**, 47007 (2010).
[25]N. Kumar, B. A. Ruzicka, N. P. Butch, P. Syers, K. Kirshenbaum, J. Paglione, and H. Zhao, Phys. Rev. B **83**, 235306 (2011).
[26]J. Qi, X. Chen, W. Yu, P. Cadden-Zimansky, D. Smirnov, N. H. Tolk, I. Miotkowski, H. Cao, Y. P. Chen, Y. Wu, S. Qiao, and Z. Jiang, Appl. Phys. Lett. **97**, 182102 (2010).
[27]W. Richter, H. Kohler, and C. R. Becker, Phys. Stat. Sol. (b) **84**, 619 (1977).
[28]J. Zhang, Z. Peng, A. Soni, Y. Zhao, Y. Xiong, B. Peng, J. Wang, M. S. Dresselhaus, and Q. Xiong, Nano Lett. **11**, 2407 (2011).
[29]M. R. Portnoff, IEEE Trans. Acoust., Speech, Signal Process. **28**, 55 (1980).
[30]A. H. Nuttall, IEEE Trans. Acoust., Speech, Signal Process. **29**, 84 (1981).
[31]A. Yabushita, T. Kobayashi, and M. Tsuda, J. Phys. Chem. B **116**, 1920 (2012).